

Open-loop glucose control: Automatic IOB-based super-bolus feature for commercial insulin pumps

Nicolás Rosales^{a,*}, Hernán De Battista^a, Josep Vehí^{b,c}, Fabricio Garelli^a

^a Grupo de Control Aplicado (GCA), Instituto LEICI, UNLP-CONICET, Facultad de Ingeniería, Universidad Nacional de La Plata, Argentina

^b Institut d'Informàtica i Aplicacions, Universitat de Girona, Campus de Montilivi, Girona, Spain

^c Centro de Investigación Biomédica en Red de Diabetes y Enfermedades Metabólicas Asociadas (CIBERDEM), Girona, Spain

ARTICLE INFO

Article history:

Received 15 December 2016

Revised 6 February 2018

Accepted 9 March 2018

Keywords:

Diabetes management

Glycemic control

Insulin-On-Board

Insulin dosing

Duration of insulin action

ABSTRACT

Background and Objective: Although there has been significant progress towards closed-loop type 1 diabetes mellitus (T1DM) treatments, most diabetic patients still treat this metabolic disorder in an open-loop manner, based on insulin pump therapy (basal and bolus insulin infusion). This paper presents a method for automatic insulin bolus shaping based on insulin-on-board (IOB) as an alternative to conventional bolus dosing.

Methods: The methodology presented allows the pump to generate the so-called super-bolus (SB) employing a two-compartment IOB dynamic model. The extra amount of insulin to boost the bolus and the basal cutoff time are computed using the duration of insulin action (DIA). In this way, the pump automatically re-establishes basal insulin when IOB reaches its basal level. Thus, detrimental transients caused by manual or *a-priori* computations are avoided.

Results: The potential of this method is illustrated via *in-silico* trials over a 30 patients cohort in single meal and single day scenarios. In the first ones, improvements were found (standard treatment vs. automatic SB) both in percentage time in euglycemia (75g meal: 81.9 ± 15.59 vs. 89.51 ± 11.95 , $\rho \approx 0$; 100g meal: 75.12 ± 18.23 vs. 85.46 ± 14.96 , $\rho \approx 0$) and time in hypoglycemia (75g meal: 5.92 ± 14.48 vs. 0.97 ± 4.15 , $\rho = 0.008$; 100g meal: 9.5 ± 17.02 vs. 1.85 ± 7.05 , $\rho = 0.014$). In a single day scenario, considering intra-patient variability, the time in hypoglycemia was reduced (9.57 ± 14.48 vs. 4.21 ± 6.18 , $\rho = 0.028$) and improved the time in euglycemia (79.46 ± 17.46 vs. 86.29 ± 11.73 , $\rho = 0.007$).

Conclusions: The automatic IOB-based SB has the potential of a better performance in comparison with the standard treatment, particularly for high glycemic index meals with high carbohydrate content. Both glucose excursion and time spent in hypoglycemia were reduced.

© 2018 Elsevier B.V. All rights reserved.

1. Introduction

Current therapies for the treatment of Type 1 diabetes mellitus (T1DM) are based on the subcutaneous insulin infusion through multiple daily injections (MDI) or via a continuous subcutaneous insulin infusion (CSII) pump. The rapid acting insulin used in the latter is administered in two ways. A basal dose is continuously pumped to deliver the insulin needed between meals and overnight, whereas bolus doses are delivered to cover the effects of meals and to correct high blood glucose levels.

Modern insulin pumps incorporate bolus advisors that help patients calculate prandial boluses, a customizable basal insulin flows

to deal with daily sensitivity changes, preventive alarms, dietary carbohydrate quantity and estimated amount of insulin-on-board (IOB) [1,2]. Although CSII treatments provide better glycemic control than conventional therapies with MDI and lower the risk of hypoglycemia, most of T1DM patients do not maintain glucose targets. High post-meal hyperglycemic excursions and late post-absorptive hypoglycemia still constitute a therapeutic challenge. In order to avoid these symptoms, some patients rely on the routine of basal insulin suspension for several hours, leaving meal bolus to cover both prandial and basal insulin requirements [3]. Also, there are both *in-silico* [4] and clinical [5] comparative studies showing better postprandial glucose control using other basal-bolus combinations than the standard one. When the basal insulin delivery is stopped or reduced during a time period and the non-delivered quantity of basal insulin is added to a meal or correction bolus, a super-bolus is created. This shift of basal to bolus insulin creates a

* Corresponding author.

E-mail address: nicolas.rosales@ing.unlp.edu.ar (N. Rosales).

larger bolus that is particularly beneficial when insulin is needed quickly. These situations may include, but are not limited to, covering high glycemic index (HGI) foods, large intakes of carbohydrate, and fast return of an elevated blood sugar to normal [2].

Recently, the first world-commercial product for hybrid glucose control has been launched in the U.S.A. market (MiniMed 670G system®, Medtronic Inc., Northridge CA). Although it represents a great advance towards fully automatic control, the feedforward action corresponding to insulin boluses must still be carried out manually. This gives an idea of the difficulty of his calculation. The work presented here is aimed at improving the delivery of insulin bolus to achieve a better trade-off between performance and safety in open-loop therapies which are, by far, the most common today. This approach allows improving current glucose control therapies as well as gaining insight into IOB constraint implications in real diabetic treatments. In particular, an algorithm that automatically shapes a super-bolus (SB) without the need of manual intervention.

The layout of the remaining part of the paper is as follows. Section 2 describes the motivation for the treatment development. Section 3 develops the main proposal of the paper. The evaluation protocol is defined in Section 4 and in Section 5 the results obtained from *in-silico* tests are presented. Discussion are drawn in Section 6 and conclusions in Section 7.

2. Motivation

The main motivation for implementing a SB treatment in glucose management is to compensate for the slow dynamic action of insulin with respect to the time at which meals raise the blood glucose.

The glucose-insulin system is a positive dynamical system, i.e. a dynamical system where all state variables and inputs are positive. The recent work [6] presents some relevant results about this

sort of systems subjected to perturbations. A critical situation appears when the disturbance pulse response peaks faster than the input pulse response. In fact, all attempts to diminish the effect of a disturbance in the output at an early time necessarily lead to undershoot at a later time. These results are obviously applicable to T1DM basal-bolus treatments where meals typically raise blood sugar before insulin acts. They allow formalizing the trade-off between hyperglycemia excursions and hypoglycemia events inherent to the insulin-glucose system limitations.

The main contribution of [6] can be summarized as follows. Consider a positive dynamical system perturbed with a pulse disturbance at $t = 0$ (e.g. T1DM model perturbed by a meal). Let T_1 and $T_2 > T_1$ be two arbitrary sample times and $y(T_1)$ and $y(T_2)$ the corresponding deviations of the system output w.r.t. its set-point. If one sets a lower bound \underline{y}_{T_2} for the output response at T_2 (e.g. a minimum acceptable postprandial glucose level), $y(T_2) > \underline{y}_{T_2}$, then the output response at time T_1 will be also lower bounded by $y(T_1) > \underline{y}_{T_1}$ (e.g. the postprandial peak will be at least \underline{y}_{T_1}). The value of \underline{y}_{T_1} will be function of the disturbance, the system dynamics and parameters and linked to the boundary set for $y(T_2)$. Although T_1 and T_2 are arbitrary, it is interesting to align them with the maximum and minimum values of the output response. This allows predicting the trade-off between positive and negative excursions of the output signal. The system input that fulfils both bounds is a pulse at $t = 0$ (at the time that the perturbation occurs) and zero elsewhere in the interval $[0, T_2]$.

These results have direct implications when applied to T1DM models. Fig. 1 illustrates their application to a basal-bolus combination to reject a meal disturbance. This response is obtained for the linearized model of adult#6 of the UVA/Padova T1DM simulator. The patient starts with a steady-state glucose of 100 mg/dl, where the basal insulin for this patient is 1.9 U/h. A 30 g CHO meal is given at $t = 0$. According to the I:C ratio of this patient,

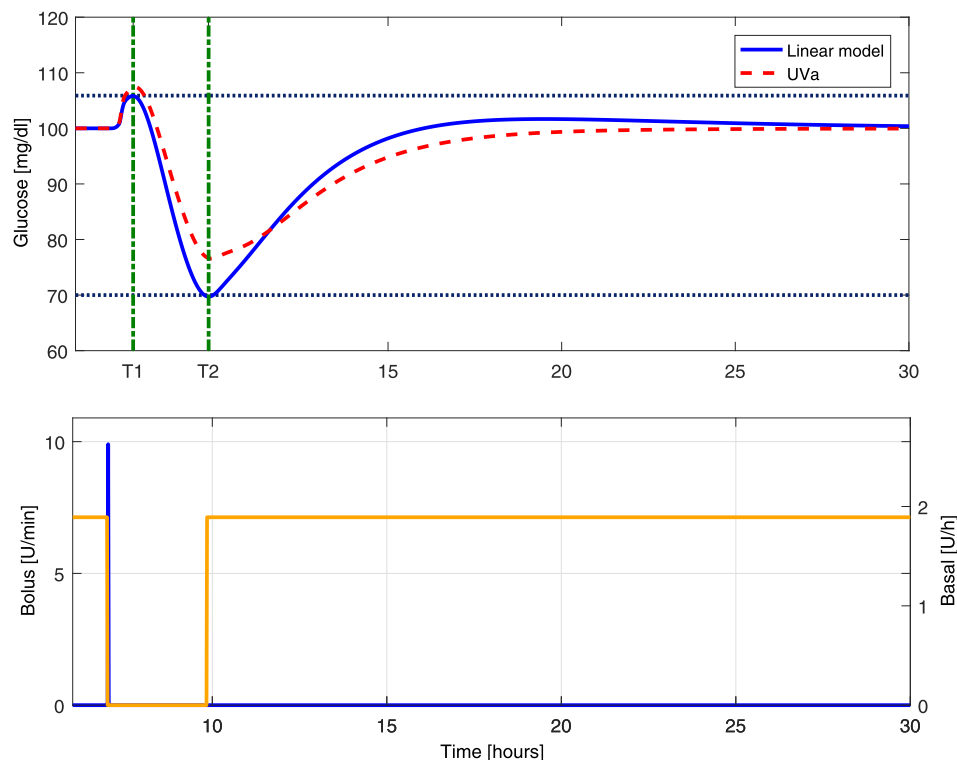


Fig. 1. Result illustrating the theoretical result of [6]. Upper panel: glucose profiles (blue solid line corresponds to the linearized patient; red dashed line corresponds to the UVa patient); dotted horizontal lines indicate the lower bounds \underline{y}_{T_1} and \underline{y}_{T_2} for T_1 and T_2 , respectively. Lower panel: insulin input (both basal and bolus) that fulfils both bounds. (For interpretation of the references to color in this figure legend, the reader is referred to the web version of this article.)

the meal bolus is three insulin units (3U). Let us assume for the moment that times $T_1 = 50$ min and $T_2 = 170$ min at which maximum and minimum glucose levels occur are known a-priori. Set the minimum acceptable glucose level $y_{T_2} = 70$ mg/dl. Then, after some computations, it can be determined that the maximum glucose level will be at least $y_{T_1} \geq 105.9$ mg/dl. Furthermore, the control input that provides the lower hyperglycemia excursion at $T_1 = 50$ min given a minimum glucose value $y_{T_2} = 70$ mg/dl at $T_2 = 170$ min is depicted at the bottom of the figure. The basal-bolus input profile consists of an insulin bolus at meal time and basal suspension until the lowest glucose level at $T_2 = 170$ min occurs. As mentioned above, this is the shape of a super-bolus, where the 9.9 U insulin bolus is much higher than the 3 U standard bolus. The extra amount of insulin administered at meal time compensates for the amount of basal insulin not delivered until T_2 . For further details the reader is referred to [6].

The previous results are very interesting from a theoretical viewpoint and provide an analytic way to determine the shape of the best input profile. However, the assumption that time instants T_1 and T_2 are known a-priori is unrealistic. Therefore, despite guaranteeing performance specifications, the method proposed in [6] cannot be used to determine the best basal-bolus combination in daily glucose management.

Nowadays the pump users usually set manually a SB treatment for some kinds of meals according to physician recommendation [2]. However, an a-priori amount of basal insulin should be removed, which may not always be correctly guessed. Indeed, one of the main open questions in diabetes forums about SB is “how long can the basal be lowered/stopped before a rebound will occur once SB is gone?”. In current commercial insulin pumps an automatic SB is not implemented yet, probably because of this open question. The automatic calculus of the SB can be addressed in different ways, from the simplest way of defining a fixed time regardless the patient to more complex forms involving clinical information of the patient as proposed in this paper.

The proposal of the automatic IOB-based SB treatment arises from finding a basal-bolus combination capable of a better glucose management. This therapy is expected to be useful when counteracting HGI meals. For this purpose, the concept IOB is used in order to compute the extra amount of insulin to boost the bolus and the time when the basal insulin delivery is re-established.

3. Methods

The idea behind the proposal comes from the methodology registered on patent and priority requests [7,8]. This idea consists in imposing a constraint over the IOB profile generated by the treatment. Since the proposed algorithm is based on the residual insulin that is still active in the body, it is here briefly recalled the main available methods to estimate IOB through mathematical models.

3.1. IOB estimation

IOB estimation is used by smart pumps to prevent from excessive insulin stacking, particularly when boluses are given close together. An individualization of IOB estimation is usually characterized by the duration of insulin action (DIA), a parameter that clinicians are used to tune when setting up insulin pumps [2]. Typically, IOB estimation can be done by means of simple discrete models like those implemented in modern insulin pumps (based on straight lines or curves), or by means of a continuous subcutaneous absorption model like those available in the literature [9–11]. Each of these models is described in the following.

Some pumps use linear plots to make the concept of IOB easier for patients to understand. The model simply describes IOB trace

Table 1

IOB model parameter K_{DIA} (min^{-1}) for different durations of insulin action.

DIA (h)	2	3	4	5	6	7	8
$K_{DIA} \times 10^{-3}$	39	26	19.5	16.3	13	11.3	9.9

as

$$IOB(T_k) = I_{bolus} \cdot \left(1 - \frac{(T_k - T_{bolus})}{DIA} \right), \tag{1}$$

where I_{bolus} is the total amount of insulin supplied in a previous bolus, T_k is the current time in minutes, T_{bolus} is the bolus time, $T = T_k - T_{bolus}$ is the time lapsed from the previous bolus, and DIA is the duration of insulin action in hours.

Although the simplest one, the problem with this model is that it is mainly thought to estimate bolus-on-board (BOB) rather than IOB, since it computes insulin absorption from discrete insulin injections (boluses). In addition, it is the model with larger error with respect to the actual IOB pattern, as it assumes a non-realistic straight line profile.

A slight improvement of the previous model implemented in some insulin pumps is based on insulin curves, from which IOB is computed as

$$IOB(T_k) = IOBcurve^T \cdot I_{past}(T_{k-1}, T_{k-N}), \tag{2}$$

where $IOBcurve^T$ is a row vector with N components (factors lower or equal than one) representing an insulin action curve, $I_{past}(T_{k-1}, T_{k-N})$ is a column vector with a record of the insulin supplied over the last DIA hours, from time T_{k-N} to time T_{k-1} , and $N = floor(DIA \cdot 60 / T_s)$, where T_s is the pumping period.

A two-compartment dynamical linear model for subcutaneous insulin absorption is used in most *in-silico* trials and control strategies validation (e.g. [12]). Indeed, this dynamic representation is used for the subcutaneous insulin absorption model in UVa/Padova T1DM simulator, which is widely described in the literature [13], given by:

$$\begin{cases} \dot{I}_{sc1} = -(k_d + k_{a1})I_{sc1} + u \\ \dot{I}_{sc2} = k_d I_{sc1} - k_{a2} I_{sc2} \end{cases} \tag{3}$$

$$IOB = I_{sc1} + I_{sc2} \tag{4}$$

where I_{sc1} and I_{sc2} are, respectively, the amount of nonmonomeric and monomeric insulin in the subcutaneous space, u is the exogenous insulin infusion rate in [pmol/min/kg], k_d [min^{-1}] is the rate constant of insulin dissociation, and k_{a1} [min^{-1}] and k_{a2} [min^{-1}] are the rate constants of nonmonomeric and monomeric insulin absorption, respectively. Although this model could also be used here to estimate the IOB, in order to minimize the parameters to be tuned, a model that can be personalized based solely on a-priori clinical information is considered, like the dynamical model presented in [9]:

$$\begin{cases} \dot{I}_{sc1} = -K_{DIA} I_{sc1} + u \\ \dot{I}_{sc2} = K_{DIA} (I_{sc1} - I_{sc2}) \end{cases} \tag{5}$$

$$IOB = I_{sc1} + I_{sc2} \tag{6}$$

In this case, only the constant K_{DIA} [min^{-1}] has to be tuned for each patient so as to replicate its corresponding DIA. Table 1 shows the values of K_{DIA} for several DIA values. This model is the more accurate of the aforementioned and allows a continuous estimation of the IOB from the insulin input.

Although a widespread confusion exists among clinicians and patients regarding the selection of an accurate DIA setting, many specialist have recently highlighted the problems that arise when

an inappropriately short DIA is set. Research protocols to accurately measure DIA have been proposed and it is recognized of great importance that insulin manufacturers verify actual DIA for rapid-acting insulins on the market [14].

Since the subcutaneous insulin absorption dynamics can change over time in patients, particularly if the Body Mass Index (BMI) changes, it is important to update the DIA regularly. Note that recent estimators based on continuous glucose monitors (CGM) readings, as the ones proposed in [15,16], could also be employed for the estimation of IOB or parameters involved in the dynamics of subcutaneous absorption model. These observers, commonly employed in closed-loop control systems, perform a real-time estimation of plasma insulin concentration, thus allowing to obtain a more accurate value of the patient's DIA.

3.2. Automatic IOB-based super bolus

To overcome the need of *a-priori* setting of the cutoff time, i.e. the time during which the basal insulin delivery is suspended when applying a SB, an automatic IOB-Based SB is proposed here.

The underlying idea of the proposal is easy and intuitive. It imposes a soft constraint on IOB that allows limiting the insulin delivered to the patient. This consists in fixing a threshold value on the IOB level \overline{IOB} . When the SB is delivered, the IOB limit value will be exceeded, so the basal supply will not resume until the IOB level reaches again the threshold constraint. As a result, insulin will not continue accumulating while IOB is above the threshold, thus avoiding or reducing possible cases of late hypoglycemia.

In order to illustrate and understand the operation of the automatic SB, a comparison between the IOB profiles generated by a manual SB and the proposed method is considered. The estimation of the IOB is obtained from the dynamic model described in the previous section, given by Eq. (5). This will be further developed in the next subsection.

Three different patients -let say A, B and C- are on steady-state under a basal rate of 1U/h. The patients have an approximated DIA of 7, 4 and 3 h, respectively. One hour into the simulation an insulin bolus of 2 U is programmed.

A manual SB with a generic fixed cutoff time of 2 h was simulated, thus creating an insulin injection of 4U. The corresponding IOB profiles and SB are shown in Fig. 2. The dotted lines indicate the \overline{IOB} for each patient. In this case, \overline{IOB} is equal to the steady-state value of the IOB for each patient. It can be seen that for patient A the basal supply returns before the \overline{IOB} has been reached by the estimated IOB, so there is insulin stacking (dashed line). A larger transient in the IOB is undesired because it can produce future low levels in glucose, even hypoglycemia. In the case of patient C, the IOB level falls under the \overline{IOB} within the cutoff time (dash-dot line), giving rise to an undesired undershoot. The IOB profile of patient B (solid line) does not present excessive insulin stacking or deficit because the basal supply returns when the IOB level is close to the basal value. This kind of profile is achieved randomly using a manual SB, since an arbitrary T_{cutoff} is selected.

The automatic IOB-based SB was simulated on the three patients under the same conditions. It can be seen in Fig. 3 that undesired transients or undershoots are avoided for the three patients since the basal supply returns when the IOB level is equal to the steady-state IOB. Even so, a small transient can be observed due to the second order dynamics of the system which can be avoided by choosing the \overline{IOB} slightly higher than the steady-state value. The subcutaneous insulin injection for each case can be seen at the bottom of Fig. 3, where it is evident how the cutoff time is adapted depending on the DIA to compensate inter-patient DIA variability.

3.2.1. Calculation criteria

The proposal allows the pump to execute an algorithm when the patient desires to inject a certain bolus in the shape of a SB. The algorithm calculates a dose of insulin $I[t]$ (basal and bolus) taking into account the estimation of IOB according to the following methodology:

$$I[t] = I_{basal}[t] + I_{SB}[t], \quad (7)$$

with basal infusion given by

$$I_{basal}[t] = \begin{cases} 0 & \text{if } T_{bolus} \leq t \leq T_{bolus} + T_{cutoff} \\ BR[t]T_s & \text{else} \end{cases}, \quad (8)$$

and at the time of the bolus injection a super bolus

$$I_{SB}[t] = \begin{cases} I_{bolus} + \bar{I}_b & \text{if } t = T_{bolus} \\ 0 & \text{else} \end{cases} \quad (9)$$

where:

- $I[t]$ is the total dose of insulin (in insulin units U)
- $BR[t]$ is the patient's basal rate profile (in insulin units per minute U/min)
- T_s is the sampling time
- \bar{I}_b is the sum of the basal insulin given between T_{bolus} and $T_{bolus} + T_{cutoff}$, expressed by Eq. (10)

$$\bar{I}_b = \sum_{k=T_{bolus}/T_s}^{(T_{bolus}+T_{cutoff})/T_s} BR[k] \cdot T_s \quad (10)$$

The value of the original carb bolus to be administered I_{bolus} can be computed as usual based on the insulin-carbohydrate ratio (I:CHO) of the user and the magnitude of the meal that the user will ingest (grams of carbohydrates), or via any other method.

The basal infusion will depend on an imposed IOB constraint $\overline{IOB}[t]$. The time during which the basal insulin infusion will be interrupted can be predicted from the dynamic response of the IOB system due to an input in the shape of a SB given by (7). A discrete realization sampled at $t = kT_s$ of the validated model (5) is used for the estimation of the IOB:

$$x[k+1] = A x[k] + Bu[k] \quad (11)$$

$$IOB[k] = C x[k]$$

with

$$A = \begin{bmatrix} (1 - K_{DIA} \cdot T_s) & 0 \\ K_{DIA} \cdot T_s & (1 - K_{DIA} \cdot T_s) \end{bmatrix}, \\ B = \begin{bmatrix} T_s \\ 0 \end{bmatrix}, \\ C = [1 \quad 1]. \quad (12)$$

It is desired to calculate the IOB profile after the SB delivery. The trajectories of the states $x[k]$ at each sample can be expressed by the solution to the non-homogeneous linear time invariant system (11) as

$$x[k] = A^{k-k_0} x_0 + \sum_{\tau=k_0}^{k-1} A^{k-1-\tau} Bu[\tau], \quad (13)$$

where the input bolus is defined by Eq. (9), re-written as

$$u[k] = \begin{cases} I_{SB} & \text{if } k = k_0 \\ 0 & \text{else} \end{cases} \quad (14)$$

Considering $T_{bolus} = t_0 = k_0 T_s$, the trajectories of $x[t]$ from t_0 to $t_0 + T_{cutoff}$ can be computed from the homogeneous response due

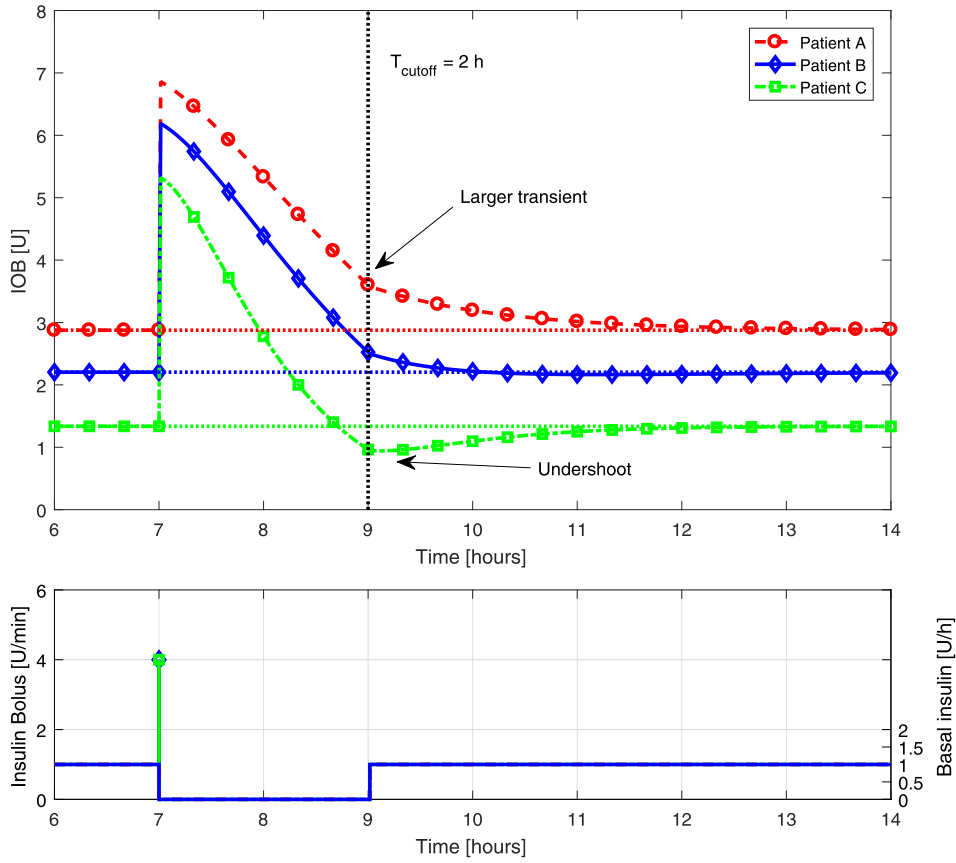


Fig. 2. IOB profiles for different patients with a manually implemented SB.

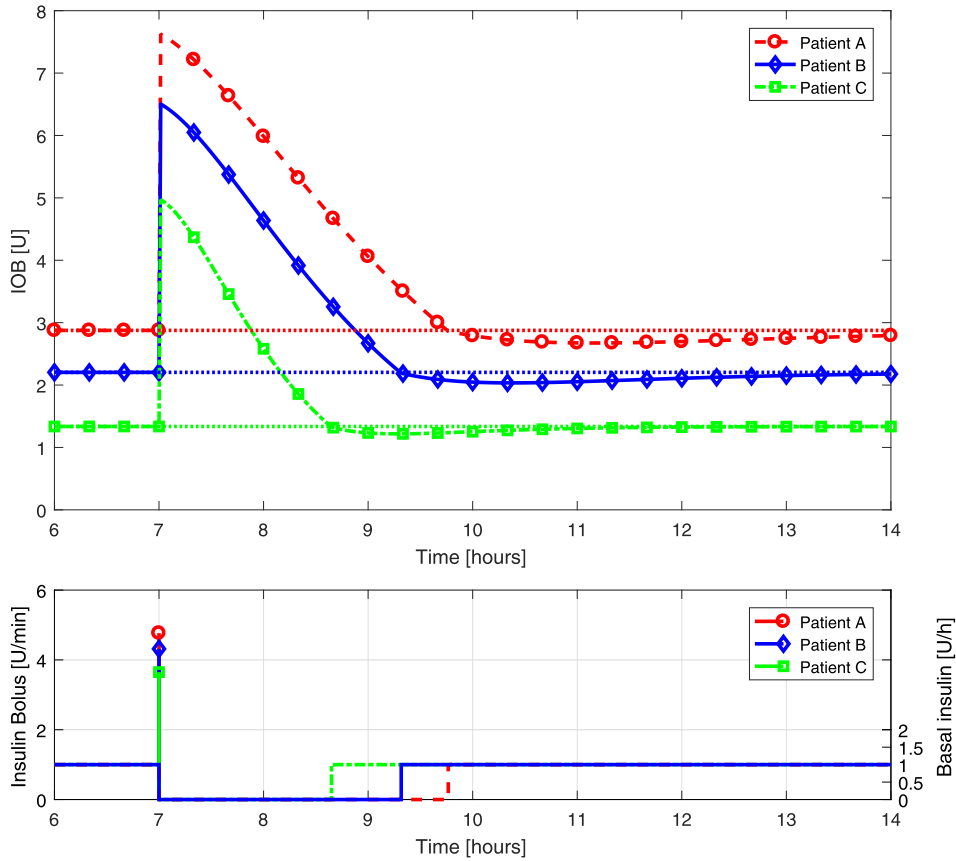


Fig. 3. IOB profiles for different patients with the automatic IOB-based SB.

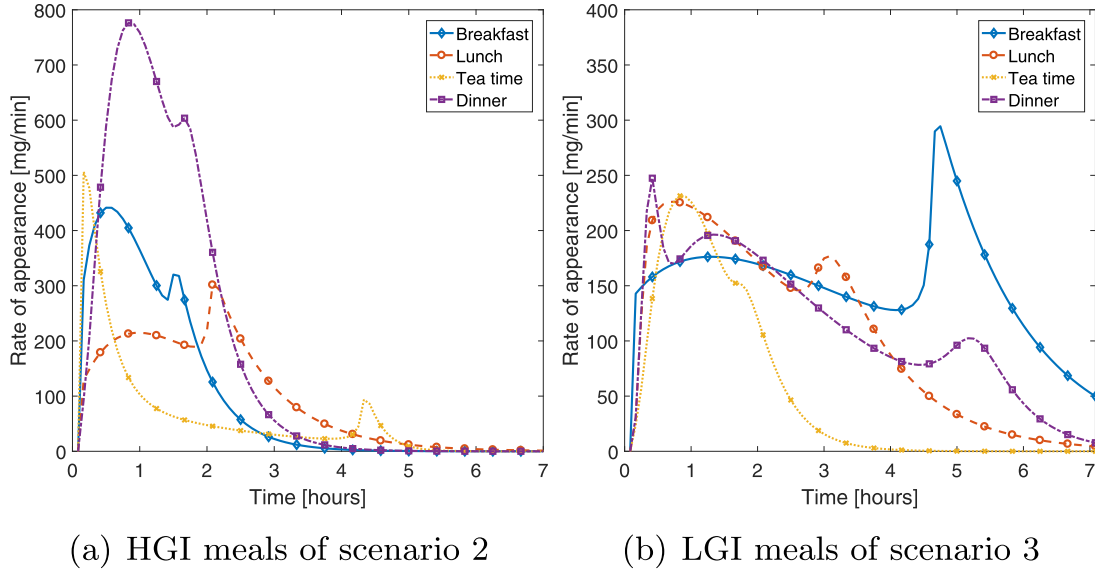


Fig. 4. Mean rate of glucose appearance of the mixed meals used in scenario 2 and 3.

to the interruption of basal delivery and the forced response due to the input (14)

$$\chi[t_0 + T_{cutoff}] = A^{T_{cutoff}/T_s} \chi_0 + A^{T_{cutoff}/T_s - 1} B \cdot I_{SB}, \quad (15)$$

where χ_0 is the states values at T_{bolus} , and the estimated IOB results

$$IOB[t_0 + T_{cutoff}] = CA^{T_{cutoff}/T_s} \chi_0 + CA^{T_{cutoff}/T_s - 1} B \cdot I_{SB} \quad (16)$$

Although the method allows selecting any $\overline{IOB}[t]$, it is proposed here to use the steady-state or basal IOB value IOB_{basal} to avoid unnecessary undershoots or delays in the IOB signal as illustrated above. So, when the basal delivery resumes, the insulin remaining in the body will be equal to the steady-state of (11) due to the basal insulin profile at $T_{bolus} + T_{cutoff}$. i.e.

$$IOB_{basal} = 2 \cdot BR[T_{bolus} + T_{cutoff}] / K_{DIA}. \quad (17)$$

Finally, the computation of T_{cutoff} and the extra amount of bolus I_b to be applied results from solving the equation

$$IOB_{basal} = CA^{T_{cutoff}} \chi_0 + CA^{T_{cutoff} - T_s} B \left(I_{bolus} + \sum_{t=0}^{T_{cutoff}} BR[t] \cdot T_s \right) \quad (18)$$

Table 2
Comparison of the standard treatment with the automatic SB for single meal scenarios.

	Mean BG (mg/dl)	BG < 50 mg/dl (%time)	BG < 60 mg/dl (%time)	BG < 70 mg/dl (%time)	BG ∈ [70,180]mg/dl (%time)	BG > 180 mg/dl (%time)	BG > 250 mg/dl (%time)	BG > 300 mg/dl (%time)
<i>Single meal: 25 g</i>								
Standard	135.43 ± 12.48	0 ± 0	0 ± 0	0.6 ± 3.27	96.03 ± 6.82	3.37 ± 6.33	0.27 ± 1.49	0 ± 0
Automatic SB	136.46 ± 6.83	0 ± 0	0 ± 0	0.32 ± 1.75	97.72 ± 5.21	1.96 ± 5.03	0.15 ± 0.84	0 ± 0
ρ - value	0.517	–	–	0.5	0*	0.001*	0.5	–
<i>Single meal: 50 g</i>								
Standard	132.66 ± 24.25	0 ± 0	1.16 ± 6.33	2.13 ± 10.46	89.67 ± 12.27	8.2 ± 8.61	1.23 ± 4.33	0.39 ± 2.15
Automatic SB	134.92 ± 15.5	0 ± 0	0 ± 0	0.42 ± 1.65	93.53 ± 8.32	6.05 ± 8.31	0.86 ± 3.64	0.3 ± 1.62
ρ - value	0.066	–	0.5	0.5	0	0.001*	0.063	0.5
<i>Single meal: 75 g</i>								
Standard	131.15 ± 35.88	1.15 ± 6.28	2.51 ± 9.75	5.92 ± 14.48	81.9 ± 15.59	12.18 ± 9.94	3.03 ± 5.73	1.25 ± 4.31
Automatic SB	134.22 ± 25.61	0 ± 0	0.28 ± 1.54	0.97 ± 4.15	89.51 ± 11.95	9.51 ± 9.94	2.4 ± 5.05	0.95 ± 3.8
ρ - value	0.017*	0.5	0.125	0.008*	0*	0*	0.002*	0.063
<i>Single meal: 100 g</i>								
Standard	131.45 ± 47.26	3.37 ± 10.15	6.2 ± 14.31	9.5 ± 17.02	75.12 ± 18.23	15.38 ± 11.26	4.77 ± 7.15	2.62 ± 5.31
Automatic SB	135.34 ± 35.93	0.76 ± 4.15	1.14 ± 5.5	1.85 ± 7.05	85.46 ± 14.96	12.68 ± 11.76	3.77 ± 6.26	2.09 ± 4.88
ρ - value	0.011*	0.031*	0.008*	0.002*	0*	0*	0.003*	0.002*

*Statically significant ($\rho < 0.05$)

This equation can be solved numerically, e.g. via the Newton-Raphson method which converges quickly and has a low computational cost, among others.

It is worth emphasizing that this computation can be easily performed by software in any modern commercially available pump. The accuracy of the method depends both on the pump discretization -since it will inherit the physical features of each pump- and the DIA estimation. The computation speed depends on the pump's hardware and is independent of the measurement-based DIA update. In this way, SB could be added as an extra option of bolus administration only depending on the patient's DIA and his basal profile. Also this technique can be combined with the subtraction of the IOB excess from the bolus or any other method involving IOB constraints (e.g. [17]). The algorithm can be implemented with some safety considerations, as ask for confirmation by the patient of the amount of insulin and cutoff time, limiting the cutoff time to a maximum desired, among other aspects that seem necessary.

4. In-silico protocol

In order to assess the performance of the proposed open-loop treatment, a series of *in-silico* tests were performed over a simula-

tion platform developed by our group based on the T1DM model of Dalla Man et al. broadly used in literature [18]. To evaluate the performance of the algorithm, a comparison with the standard basal-bolus treatment was considered.

4.1. In-silico evaluation of single meal scenarios

In a first instance, a set of *in-silico* tests were performed over the T1DM UVa/Padova virtual patient cohort of 10 adults, 10 adolescents and 10 children within four different single meal scenarios. Each scenario consisted in one high glycemic index (HGI) meal of pure carbohydrate, provided to the patient at $t = 7$ h in a 10 h simulation. The patients start with an initial steady-state equal to their fasting glucose value and insulin basal rate that keeps the patient at its fasting glucose level. The glucose absorption evolves according Dalla Man’s model described in [18]. The sizes of the meals were 25 g, 50 g, 75 g and 100 g, respectively. A manual SB is also considered for comparison. Since there is not a standard way of defining the SB, a fixed cutoff time was considered for each meal. This fixed cutoff times were defined as the mean value between the cutoff times of the whole cohort obtained by the automatic SB treatment. The resulting cutoff times for the 25, 50, 70 and 100 g meals were 135, 166, 186 and 200 min, respectively.

4.2. In-silico evaluation of single day scenarios under intra-day variability

To evaluate the robustness of the proposed methodology, three single day scenarios were considered introducing intra-patient variability.

4.2.1. Scenario 1

A single day *in-silico* scenario was proposed for the whole patient cohort. Four HGI meals were considered at 7, 13, 17 and 21 h containing 80 g, 40 g, 10 g and 70 g of CHO, respectively. Here the patients were simulated under non-ideal and varying basal profiles and I:CHO factors.

In order to take into account a more realistic scenario, diurnal variability of the system parameters that describe insulin sensitivity (IS) (V_{mx} , k_{p3}) and glucose absorption (k_{abs} , k_{min} , k_{max}) was considered, following the work of Visentin et al. [19,20]. This way, the platform resembles the one presented by Toffanin et al. [21]. The intra-day variability for the time-varying parameters of IS and glucose absorption was implemented as an almost step-wise-line signal that varies three times a day: at 4, 11 and 17 h Each *in-silico* subject was randomly assigned to a time-varying IS class profile, as presented in [19]. The parameters involved with IS varied between 100 and 60% with a multiplicative random noise, described

by a normal distribution $N(\mu, \sigma)$, with $\mu = 1$ and $\sigma = 0.2$. The glucose absorption parameters were affected by a multiplicative random noise, using the average relative differences from [20] and described by a normal distribution $N(\mu, \sigma)$, with $\mu = 1.059$ and $\sigma = 0.044$. To take into account short-term variations on the DIA, a sinusoidal variation of 20% of amplitude and 24 h period in the subcutaneous insulin absorption parameters (k_d , k_{a1} , k_{a2}) was also considered [22,23].

Daily patterns of time-varying basal insulin rate and I:CHO ratio to compensate subject’s IS pattern were defined. The basal rate of the patients was adjusted to maintain in steady state their fasting glucose, so two levels were set: one when the IS parameters are at 100% and another when they are at 60%. The noise was not considered for the basal insulin computation. The change of basal rate is produced two hours before the change of sensitivity was defined. The different I:CHO for each moment of the day were defined as 100% or 60% of the nominal value as well, depending on the class type.

4.2.2. Scenarios 2 and 3

In addition, two scenarios are proposed including mixed meals, in order to evaluate the effect of different rates of glucose appearance and to compare the automatic SB performance when facing both HGI and LGI meals. The intra-day variability introduced in IS and in the subcutaneous insulin absorption parameters was maintained as in scenario 1.

A mixed meal library was built by using the method for glucose rate estimation reported in [24,25]. The library contains 60 meals curves with different composition, covering a great variability of glucose absorption profiles. There is the limitation that the mixed meal library comes from clinical studies performed on non-diabetic subjects, so they may have differences regarding real-life meals or less physiological responses in comparison with the glucose absorption model. Nevertheless, it is of interest testing the proposed method under mixed meals, since the glucose appearance rates could be a bigger challenge and slower rates can be considered. Moreover, according to the literature [18–20,24], the parameter variability obtained in the glucose absorption model is mostly attributed to different meal compositions.

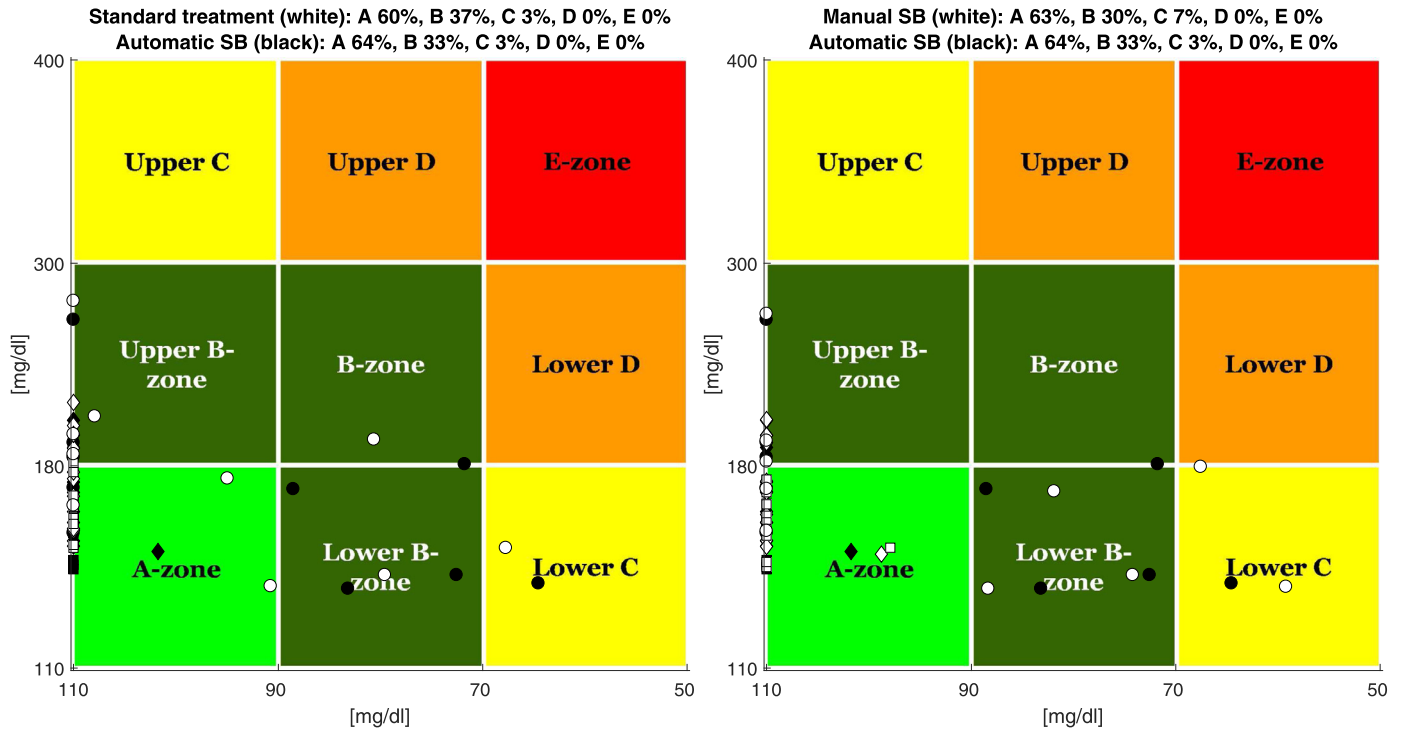
Since the glucose absorption model parameters used in the T1DM model and described in [18] were obtained from rapid absorption meals, the glucose rate of appearance profile from the library replaces the glucose absorption model of the T1DM subject. In order to enlarge the inter-patient variability, the glucose rate of appearance from the library was modulated by a random factor (both on duration and amplitude without affecting the area) and also divided by the patient’s body weight for each subject.

The two scenarios consisted in four mixed meals of a total sum of 200 g within 30 h. The time of the meals were: breakfast at

Table 3
Comparison of the standard treatment with the automatic SB for single day scenarios.

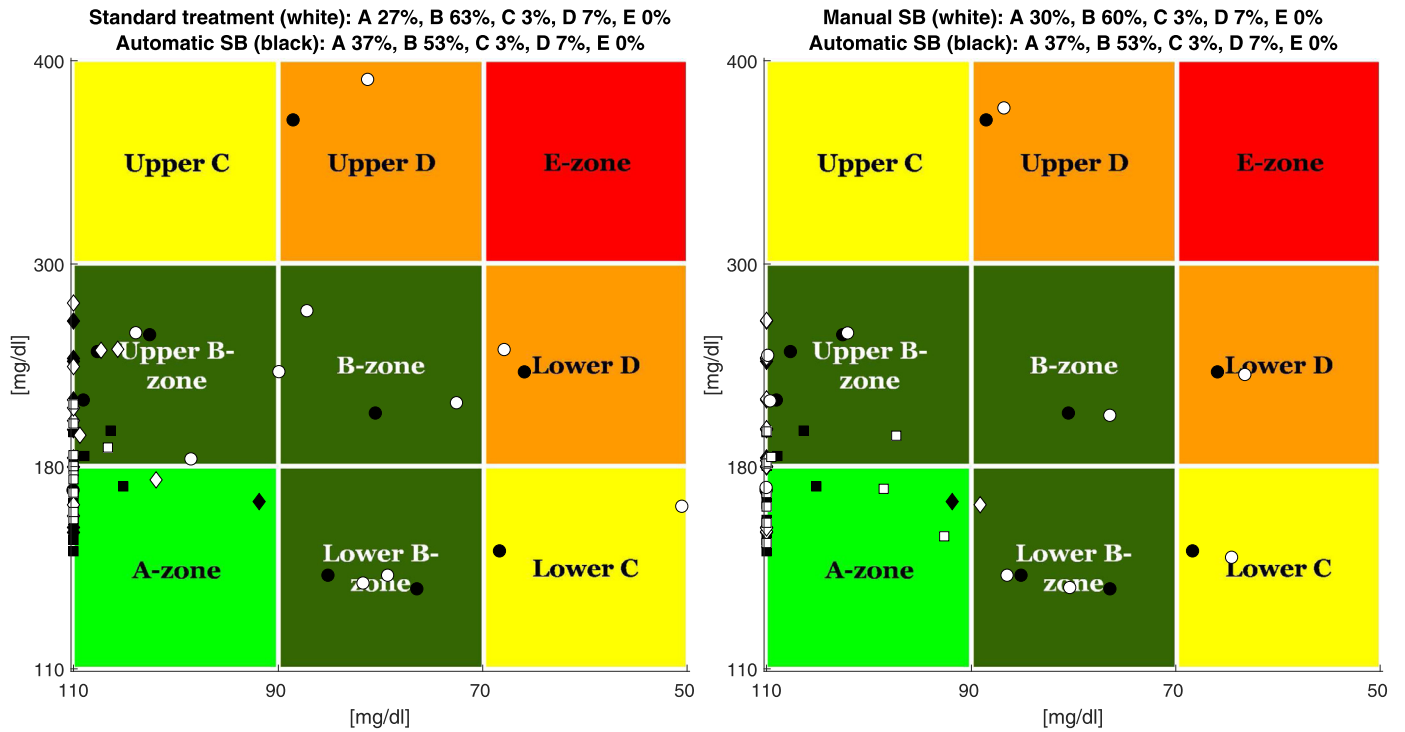
	Mean BG (mg/dl)	BG < 50 mg/dl (%time)	BG < 60 mg/dl (%time)	BG < 70 mg/dl (%time)	BG ∈ [70,180]mg/dl (%time)	BG > 180 mg/dl (%time)	BG > 250 mg/dl (%time)	BG > 300 mg/dl (%time)
<i>Scenario 1</i>								
Standard	127.45 ± 30.49	3.79 ± 7.52	6.37 ± 11.65	9.57 ± 14.48	79.46 ± 17.46	10.97 ± 10.91	2.45 ± 4.85	1.04 ± 3.15
Automatic SB	133 ± 23.56	0.44 ± 1.43	1.9 ± 4.05	4.21 ± 6.18	86.29 ± 11.73	9.5 ± 10.3	2.15 ± 5.03	0.84 ± 3.7
ρ - value	0.229	0.007*	0.008*	0.028*	0.007*	0.3	0.57	0.563
<i>Scenario 2</i>								
Standard	117.56 ± 36.94	1.2 ± 2.4	3.82 ± 5.82	9.21 ± 6.6	80.52 ± 7.94	10.27 ± 3.95	0.17 ± 0.54	0 ± 0
Automatic SB	117.25 ± 31.5	0.67 ± 1.45	2.74 ± 4.63	5.99 ± 6.48	86.23 ± 9.2	7.78 ± 4.92	0.07 ± 0.21	0 ± 0
ρ - value	0.432	0.125	0.063	0.004*	0.001*	0.001*	0.5	–
<i>Scenario 3</i>								
Standard	117.96 ± 12.05	0 ± 0	0 ± 0	0.45 ± 1.42	99.55 ± 1.42	0 ± 0	0 ± 0	0 ± 0
Automatic SB	120.35 ± 10.76	0 ± 0	0 ± 0	0.47 ± 1.47	99.04 ± 1.59	0.49 ± 0.93	0 ± 0	0 ± 0
ρ - value	0.014*	–	–	–	–	–	–	–

*Statically significant ($\rho < 0.05$)



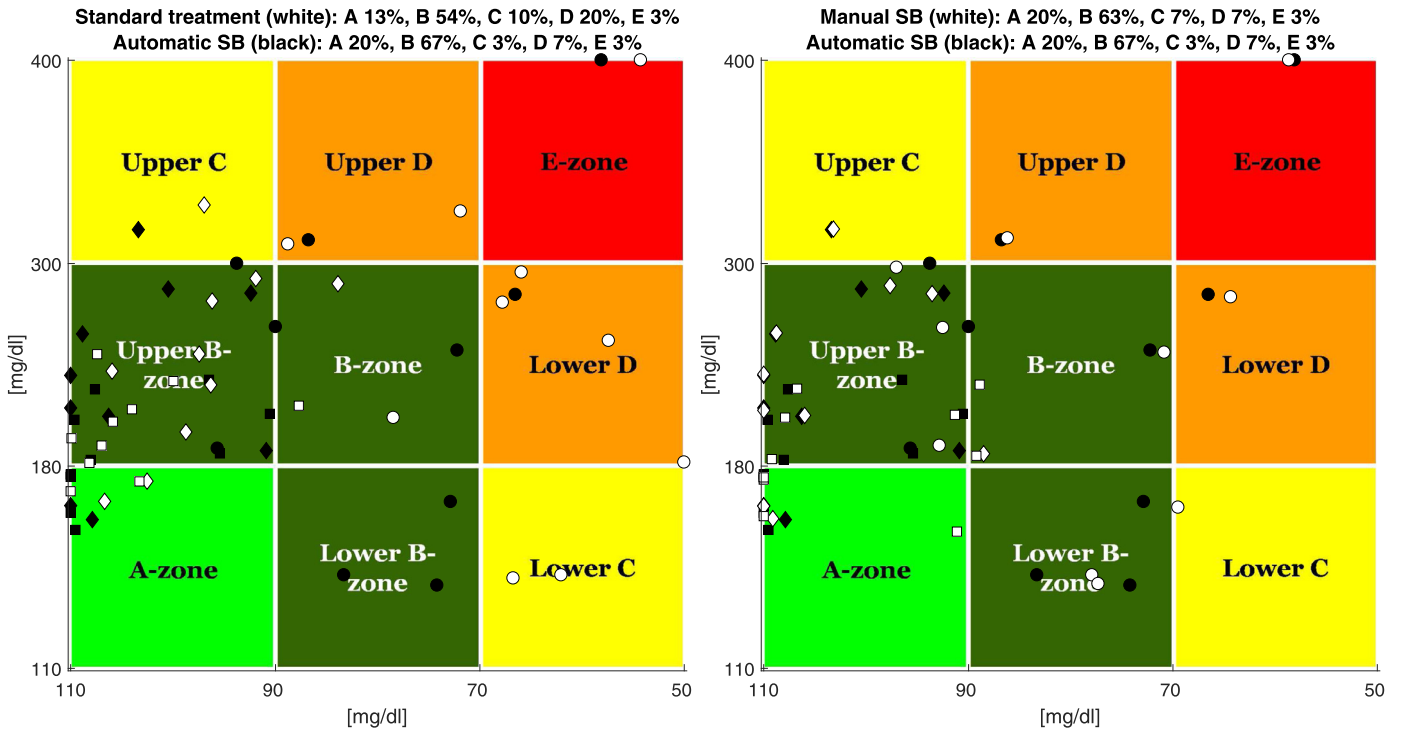
(a) Standard treatment (white markers) vs. (b) Manual SB (white markers) vs. Automatic SB (black markers)

Fig. 5. CVGA for 25g single meal scenario. Comparison between treatments in adults (square markers), adolescents (diamond markers) and children (circle markers).



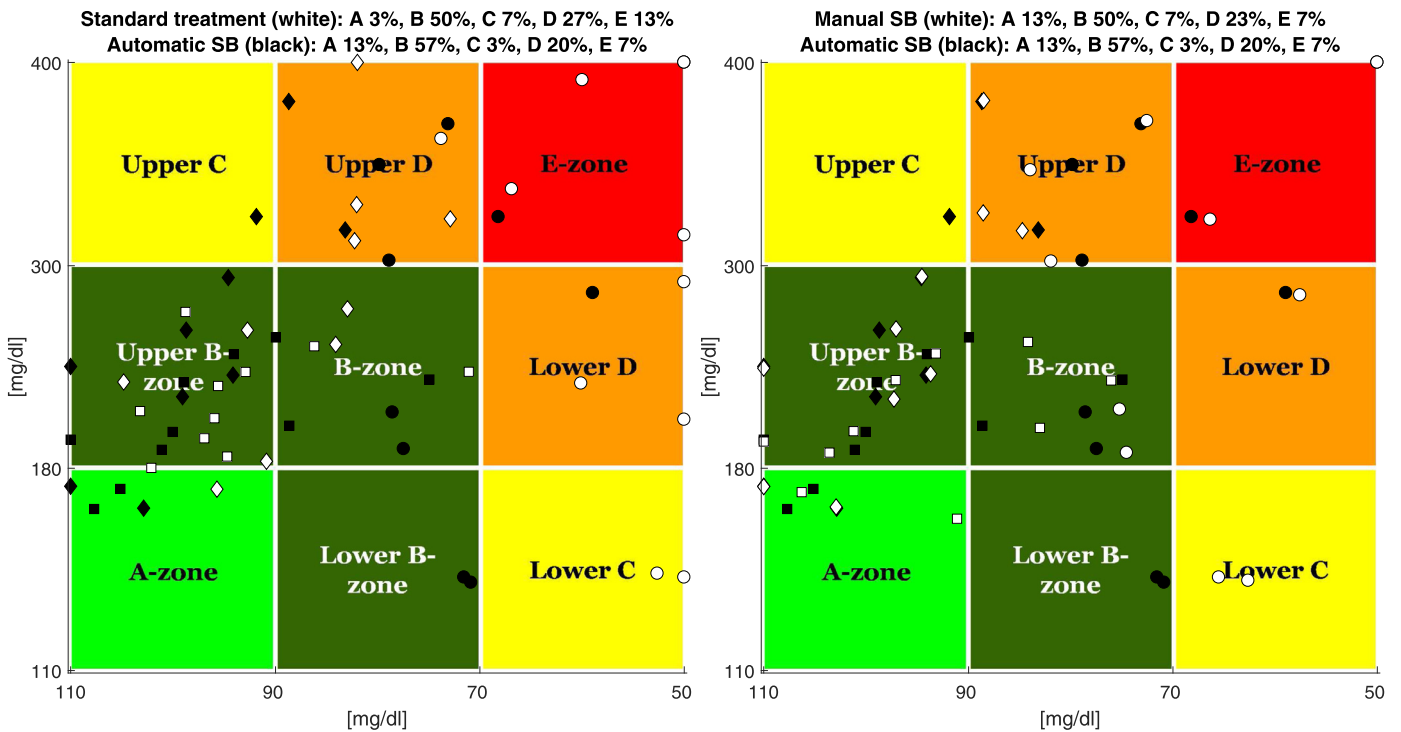
(a) Standard treatment (white markers) vs. (b) Manual SB (white markers) vs. Automatic SB (black markers)

Fig. 6. CVGA for 50 g single meal scenario. Comparison between treatments in adults (square markers), adolescents (diamond markers) and children (circle markers) for the 50 g meal.



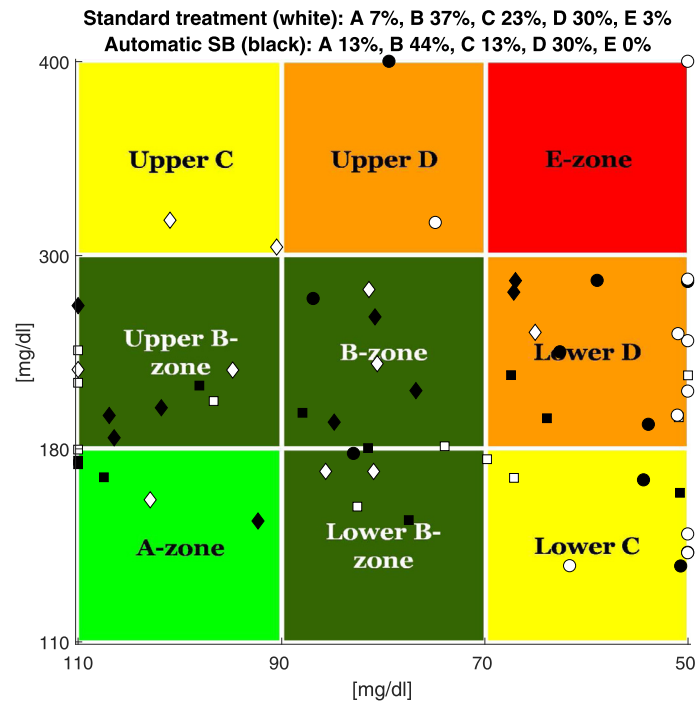
(a) Standard treatment (white markers) vs. (b) Manual SB (white markers) vs. Automatic SB (black markers)

Fig. 7. CVGA for 75 g single meal scenario. Comparison between treatments in adults (square markers), adolescents (diamond markers) and children (circle markers) for the 70g meal.

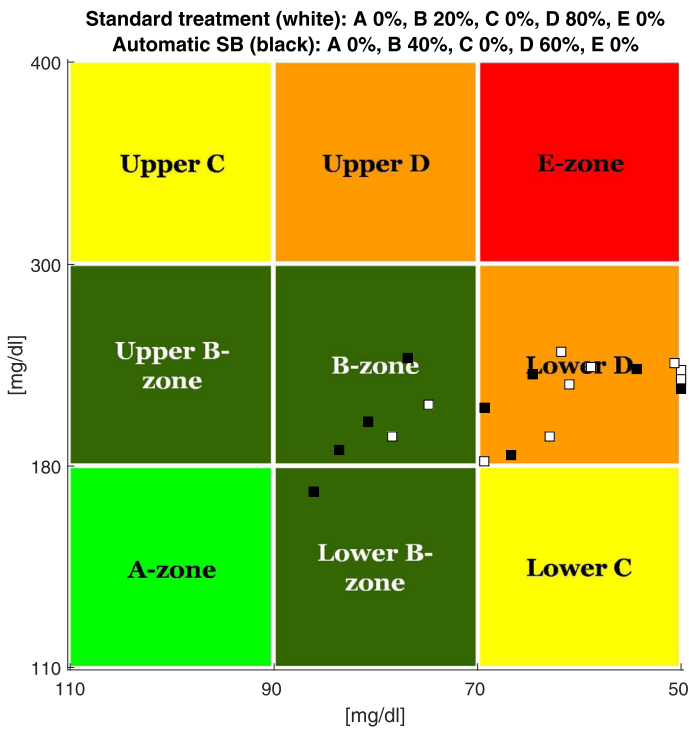


(a) Standard treatment (white markers) vs. (b) Manual SB (white markers) vs. Automatic SB (black markers)

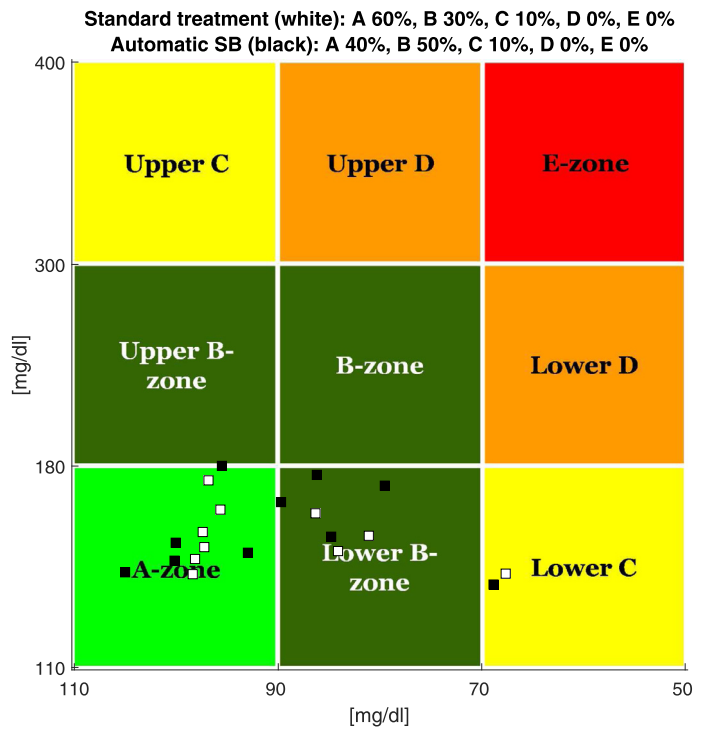
Fig. 8. CVGA for 100 g single meal scenario. Comparison between treatments in adults (square markers), adolescents (diamond markers) and children (circle markers) for the 100 g meal.



(a) Scenario 1



(b) Scenario 2



(c) Scenario 3

Fig. 9. CVGA for single day scenarios. Comparison between standard treatment (white markers) and automatic SB (black markers) (adults (square markers), adolescents (diamond markers) and children (circle markers)).

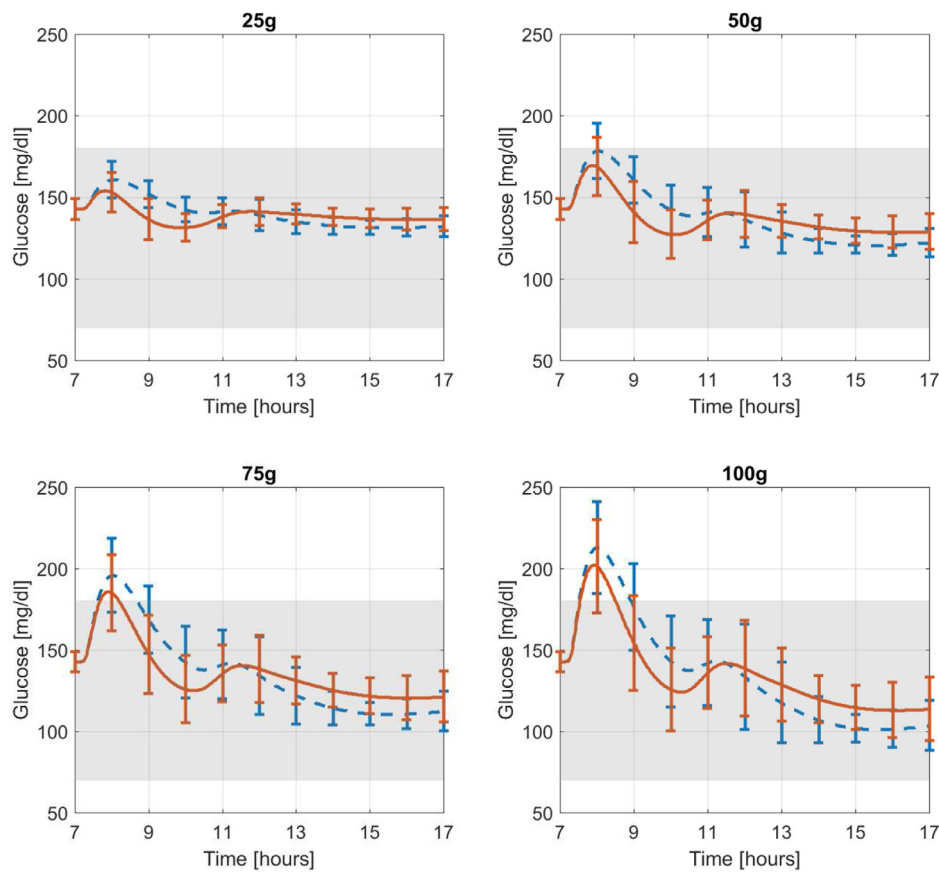


Fig. 10. Mean glucose \pm SD response of the 10 adults on single meal scenarios. Dashed-blue line corresponds to standard treatment, solid-orange line to automatic SB. Grey area indicates euglycemic range [70 – 180] mg/dl. (For interpretation of the references to colour in this figure legend, the reader is referred to the web version of this article.)

7 h, lunch at 13 h, snack at 17 h and dinner at 21h. The mean rate of glucose appearance profiles of the meals from the library are reported in Fig. 4. Fig. 4 (a) corresponds to the HGI meals of the scenario 2 and Fig. 4 (b) corresponds to the LGI meals of scenario 3.

5. Results

The evaluation metrics are presented in Tables 2 and 3, based on the consensus report [26]. For comparison between treatments, hypothesis testing was done using a 2-sample Wilcoxon Signed Rank test, considering $\rho < 0.05$ as statistically significant. In Figs. 5–8 the results for the single meal scenarios are displayed using the Control Variability Grid Analysis (CVGA) [27] plots for qualitative analysis of the control quality. For the latter, the treatments are distinguished by color and the population age by shape, being squares for adults, diamonds for adolescents and circles for children. The corresponding CVGA for the single day scenarios are shown in Fig. 9. The comparison between the mean glucose profile plus standard deviation (SD) obtained by the treatments for adults (Fig. 10), adolescents (Fig. 11) and children (Fig. 12) are shown for different carbohydrate contents. The single day scenarios mean glucose profile are shown in Fig. 13. The shadowed area indicates blood glucose (BG) euglycemic range ($BG \in [70 - 180]$ mg/dl).

6. Discussion

In summary, in the single meal scenarios the proposed method statistically improved the percentage time in euglycemia (standard treatment vs. automatic SB) (25 g meal: 96.03 ± 6.82 vs.

97.72 ± 5.21 , $\rho \approx 0$; 50 g meal: 89.67 ± 12.27 vs. 93.53 ± 8.32 , $\rho \approx 0$; 75 g meal: 81.9 ± 15.59 vs. 89.51 ± 11.95 , $\rho \approx 0$; 100 g meal: 75.12 ± 18.23 vs. 85.46 ± 14.96 , $\rho \approx 0$) and reduced the percentage time in hypoglycemia (i.e. $BG < 70$ mg/dl) (75 g meal: 5.92 ± 14.48 vs. 0.97 ± 4.15 , $\rho = 0.008$; 100 g meal: 9.5 ± 17.02 vs. 1.85 ± 7.05 , $\rho = 0.002$), the percentage time at $BG < 60$ mg/dl (100 g meal: 6.2 ± 14.31 vs. 1.14 ± 5.5 , $\rho = 0.008$) and the percentage of time hyperglycemia (i.e. $BG > 180$ mg/dl) (25 g meal: 3.37 ± 6.33 vs. 1.96 ± 5.03 , $\rho = 0.001$; 50 g meal: 8.2 ± 8.61 vs. 6.05 ± 8.31 , $\rho = 0.001$; 75 g meal: 12.18 ± 9.94 vs. 9.51 ± 9.94 , $\rho \approx 0$; 100 g meal: 15.38 ± 11.26 vs. 12.68 ± 11.76 , $\rho \approx 0$). The rest of the evaluated metrics did not experience a statistically significant change but show an improvement trend.

In the CVGA plots, depicted from Fig. 5 to 8, it is noticeable that the glucose excursion was reduced under the automatic SB in comparison with the standard treatment (standard treatment vs. automatic SB) (25 g meal: A zone 60% vs. 64%; 50 g meal: A zone 27% vs. 37%; 75 g meal: A zone 13% vs. 20%; 100 g meal: 3% vs. 13%). A down-left shift trend of the total population under the automatic SB is noticed in regard to the standard basal-bolus treatment and manual SB. Despite that the treatments fail in controlling children patients for large meals in certain cases, the results indicate that SB treatment can obtain a better open-loop control quality over large meals than the standard treatment. In Fig. 10 to 12, where the glucose profiles of each case are depicted, it can be seen how the postprandial excursion is reduced under the automatic SB treatment. The postprandial peak diminished and patients reach glucose levels closer to their fasting level in the late postprandial (8 h after the meal).

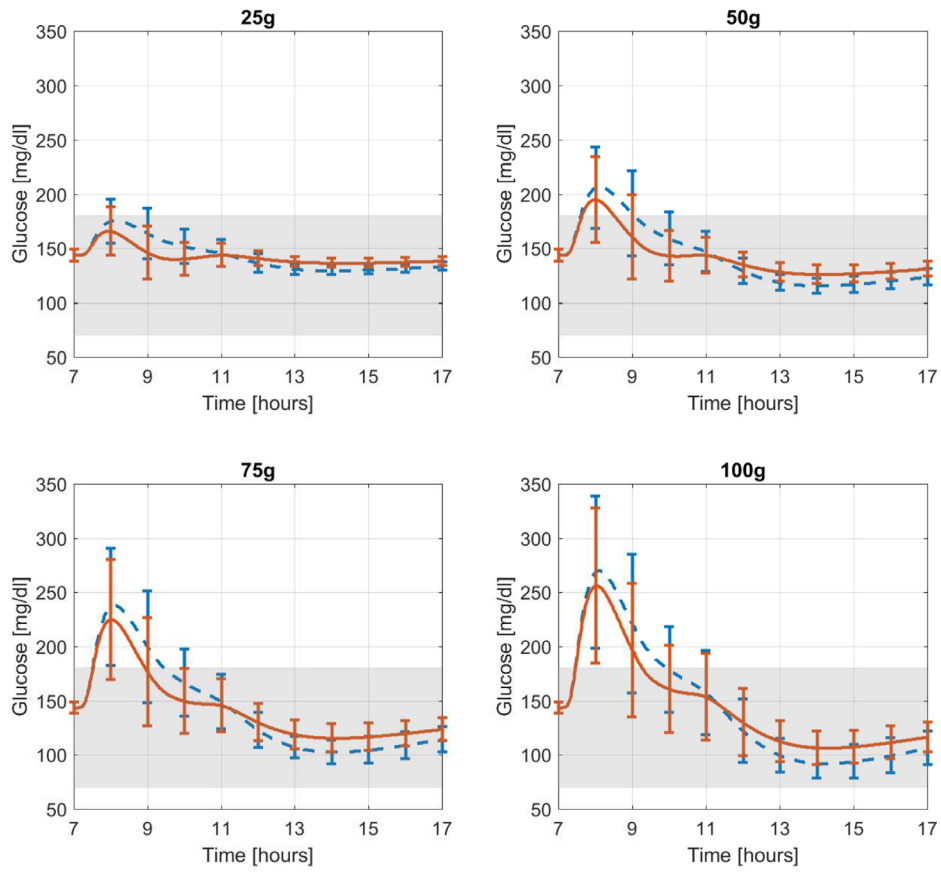


Fig. 11. Mean glucose \pm SD response of the 10 adolescents on single meal scenarios. Dashed-blue line corresponds to standard treatment, solid-orange line to automatic SB. Grey area indicates euglycemic range [70 – 180] mg/dl. (For interpretation of the references to colour in this figure legend, the reader is referred to the web version of this article.)

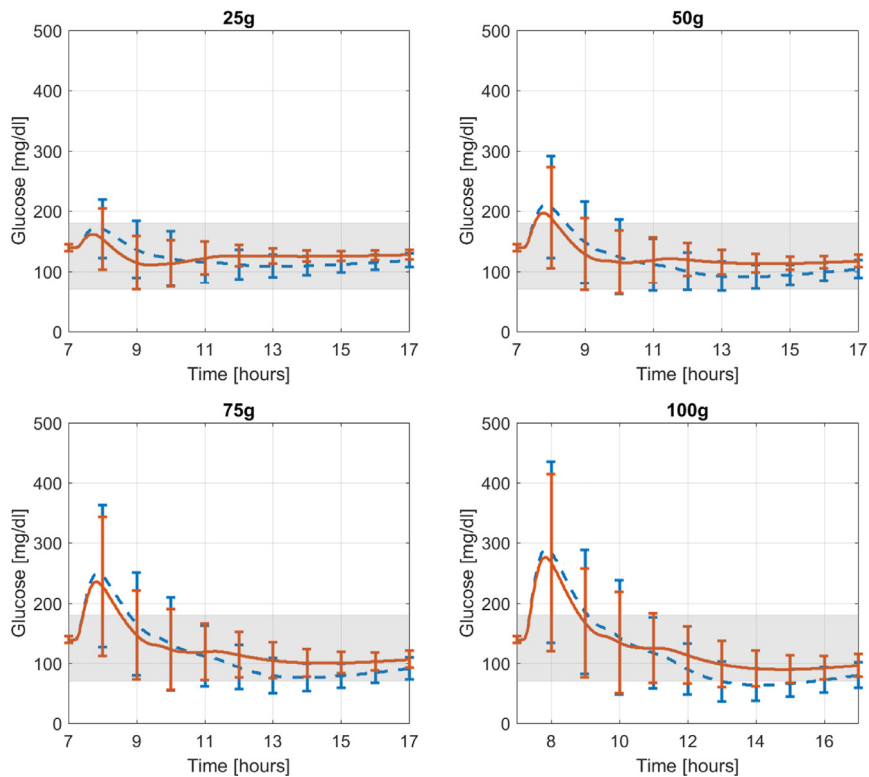
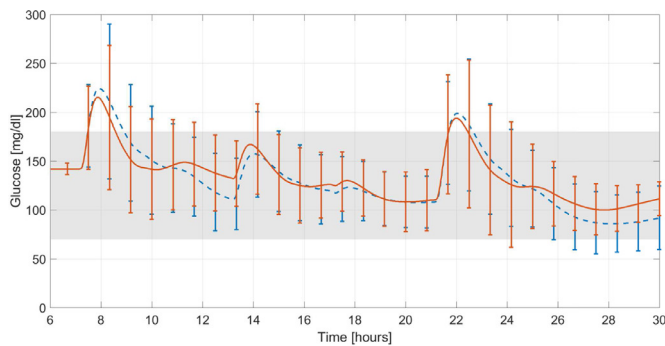
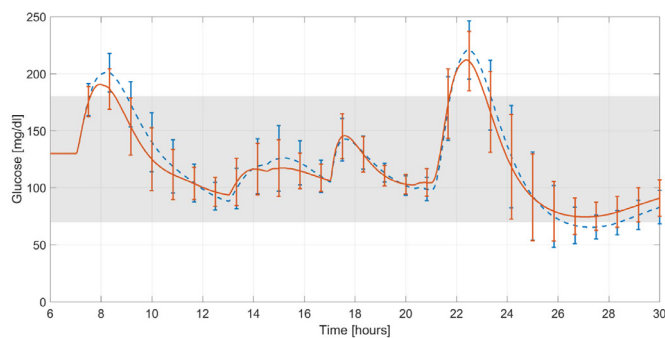


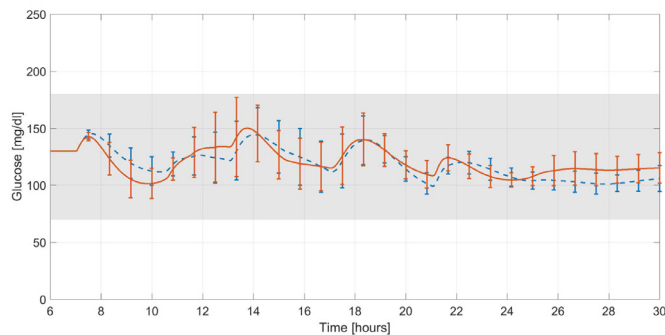
Fig. 12. Mean glucose \pm SD response of the 10 children on single meal scenarios. Dashed-blue line corresponds to standard treatment, solid-orange line to automatic SB. Grey area indicates euglycemic range [70 – 180] mg/dl. (For interpretation of the references to colour in this figure legend, the reader is referred to the web version of this article.)



(a) Scenario 1



(b) Scenario 2



(c) Scenario 3

Fig. 13. Mean glucose \pm SD profile for single day scenarios. Dashed-blue line corresponds to standard treatment, solid-orange line to automatic SB. Grey area indicates euglycemic range [70 – 180] mg/dl. (For interpretation of the references to colour in this figure legend, the reader is referred to the web version of this article.)

It is worth mentioning that the manual SB achieves a main improvement over the standard treatment as well. Still, it must be emphasized that the results obtained by the manual SB are correlated with the automatic SB since tuning of the manual SB comes from the mean of the cutoff times obtained by the proposed method. The results with the manual SB are only presented in the CVGA figures for clarity and space reasons.

Regarding the second set of simulations, in Table 3 it can be seen that the automatic SB has reduced considerably the time in hypoglycemia in Scenario 1 (9.57 ± 14.48 vs. 4.21 ± 6.18 , $\rho = 0.028$) and severe hypoglycemia ($BG < 50$ mg/dl: 3.79 ± 7.52 vs. 0.44 ± 1.43 , $\rho = 0.007$; $BG < 60$ mg/dl: 6.37 ± 11.65 vs. 1.9 ± 4.05 , $\rho = 0.008$). The time in euglycemia is improved under the automatic SB (79.46 ± 17.46 vs. 86.29 ± 11.73 , $\rho = 0.007$). Scenario 2 shows an statistically significant improvement in the percentage time spent in euglycemia (80.52 ± 7.94 vs. 86.23 ± 9.2 , $\rho = 0.001$),

hypoglycemia (9.21 ± 6.6 vs. 5.99 ± 6.48 , $\rho = 0.004$) and percentage time at hyperglycemia (10.27 ± 3.95 vs. 7.78 ± 4.92 , $\rho = 0.001$). Although the scenarios have the same total amount of carbohydrates, due to the low rate of glucose appearance of LGI meals, there is not a considerable improvement in scenario 3. In Fig. 13 it can be seen the reduction in the glucose excursion, particularly in scenarios 1 and 2. It can be remarked in Fig. 9, the reduction of the glucose excursion by the automatic SB for the first and HGI mixed meals scenarios (scenario 1: A zone 7% vs. 13%, B zone 37% vs. 44%; scenario 2: B zone 20% vs. 40%). In the case of LGI meals, the automatic SB does not show an improvement over the standard treatment. It is worth noticing in Fig. 13 (a) and (b) that the proposed method leads to glucose levels closer to target at night, after the dinner postprandial period. This result is sought in glucose management of T1DM patients because of the danger that night-time late post-absorptive hypoglycemia entails.

The methodology robustness was evaluated under conditions close to real-life scenarios and results indicate that the method improves open-loop glucose control. Even though the proposal was evaluated in an open-loop manner, using real-time estimators as mentioned, the automatic IOB-based SB could be applied in closed-loop control in order to improve glycemic control, as some current works propose [28,29].

7. Conclusion

In this work a novel treatment for open-loop glucose control was introduced, based on the SB treatment and the subcutaneous insulin dynamics of the patient. This method does not add complexity to software programming in commercial insulin pumps, giving rise to a new alternative for diabetic patients.

Despite the intrinsic limitations of being an open-loop treatment, the automatic IOB-based SB allows expecting even greater improvements in real life conditions based on the practical use and benefits of manual SB. As a whole, the results demonstrate the effectiveness of the proposed algorithm, particularly facing high HGI meals with high carbohydrate content. It is graphically noticeable in the glucose profile of each case how the postprandial glucose excursion is reduced under the automatic SB treatment, as the theoretical justification predicted.

Overall, the results of *in-silico* tests put in evidence better performance of the proposed method facing a HGI compared to the standard treatment, particularly the ones with high carbohydrate content. For HGI meals the current standard basal-bolus treatment cannot assure a good glucose control, but the automatic SB treatment may yield an improved postprandial control, being able to prevent late postprandial hypoglycemic events. The method could be implemented in the current approved devices disposing an alternative within the pump for those patients which prefer to use a SB in certain cases, so they can free themselves from the calculation and preparation of a manual SB. The *in-silico* results are good and very encouraging and worth testing the method *in-vivo*.

Conflict of interest

No competing financial interests exist.

Acknowledgment

Research in this area supported by the Argentinian Government (PICT 2014–2394, PIP 112-201501-00837 CONICET, UNLP 11/I216 and MinCyT-Colciencias CO-15-04).

References

- [1] H. Zisser, L. Robinson, W. Bevier, E. Dassau, C. Ellingsen, F. Doyle III, L. Jovanovic, Bolus calculator: a review of four “smart” insulin pumps, *Diabetes Technol. Ther.* 10 (6) (2008) 441–444.

- [2] J. Walsh, R. Roberts, *Pumping Insulin: Everything You Need for Success on a Smart Insulin Pump*, Torrey Pines Press, 2013.
- [3] M. Boronat, R.M. Sánchez-Hernández, J. Rodríguez-Cordero, A. Jiménez-Ortega, F.J. Nóvoa, Suspension of basal insulin to avoid hypoglycemia in type 1 diabetes treated with insulin pump, *Endocrinol. Diabetes Metab. Case Rep.* 1 (2015) 1–5.
- [4] A. Revert, P. Rossetti, R. Calm, J. Vehí, J. Bondia, Combining basal-bolus insulin infusion for tight postprandial glucose control: an in silico evaluation in adults, children, and adolescents, *J. Diabetes Sci. Technol.* 4 (6) (2010) 1424–1437.
- [5] P. Rossetti, F.J. Ampudia-Blasco, A. Laguna, A. Revert, J. Vehí, J.F. Ascaso, J. Bondia, Evaluation of a novel continuous glucose monitoring-based method for mealtime insulin dosing the iBolus in subjects with type 1 diabetes using continuous subcutaneous insulin infusion therapy: a randomized controlled trial, *Diabetes Technol. Ther.* 14 (11) (2012) 1043–1052.
- [6] G.C. Goodwin, A.M. Mediolì, D.S. Carrasco, B.R. King, Y. Fu, A fundamental control limitation for linear positive systems with application to type 1 diabetes treatment, *Automatica* 55 (2015) 73–77.
- [7] F. Garelli, H. De Battista, J. Vehí, F. León-Vargas, Método y programa de ordenador para la determinación y distribución temporal de una dosis de insulina a un usuario, Application INPI 20150100273, 2015.
- [8] Priority application PCT/ES2016/070051, F. Garelli, H. De Battista, J. Vehí, F. León-Vargas, Method and computer program for determination and time distribution of an insulin dose to a user, 2016.
- [9] M. Wilinska, L. Chassin, H. Schaller, L. Schaupp, T. Pieber, R. Hovorka, Insulin kinetics in type-1 diabetes: continuous and bolus delivery of rapid acting insulin, *IEEE Trans. Biomed. Eng.* 52 (1) (2005) 3–12.
- [10] J. Li, Y. Kuang, Systemically modelling the dynamics of plasma insulin in subcutaneous injection of insulin analogues for type 1 diabetes, *Math. Biosci. Eng.* 6 (1) (2009) 41–58.
- [11] G. Nucci, C. Cobelli, Models of subcutaneous insulin kinetics. a critical review, *Comput. Methods Progr. Biomed.* 62 (2000) 249–257.
- [12] M. Wilinska, L. Chassin, C. Acerini, J. Allen, D. Dunger, R. Hovorka, Simulation environment to evaluate closed-loop insulin delivery systems in type 1 diabetes, *J. Diabetes Sci. Technol.* 4 (1) (2010) 132–144.
- [13] B. Kovatchev, M. Breton, C.D. Man, C. Cobelli, In silico preclinical trials: a proof of concept in closed-loop control of type 1 diabetes, *J. Diabetes Sci. Technol.* 3 (1) (2009) 44–55.
- [14] J. Walsh, R. Roberts, L. Heinemann, Confusion regarding duration of insulin action: a potential source for major insulin dose errors by bolus calculators, *J. Diabetes Sci. Technol.* 8 (1) (2014) 170–178.
- [15] D. De Pereda, S. Romero-Vivo, B. Ricarte, P. Rossetti, F.J. Ampudia-Blasco, J. Bondia, Real-time estimation of plasma insulin concentration from continuous glucose monitor measurements, *Comput. Methods Biomech. Biomed. Eng.* 19 (1) (2016) 1–9.
- [16] I. Hajizadeh, M. Rashid, K. Turksoy, S. Samadi, J. Feng, N. Frantz, M. Sevil, E. Cengiz, A. Cinar, Plasma insulin estimation in people with type 1 diabetes mellitus, *Ind. Eng. Chem. Res.* 56 (35) (2017) 9846–9857.
- [17] P. Herrero, P. Pešl, J. Bondia, M. Reddy, N. Oliver, P. Georgiou, C. Toumazou, Method for automatic adjustment of an insulin bolus calculator: in silico robustness evaluation under intra-day variability, *Comput. Methods Progr. Biomed.* 119 (1) (2015) 1–8.
- [18] C.D. Man, R. Rizza, C. Cobelli, Meal simulation model of the glucose-insulin system, *IEEE Trans. Biomed. Eng.* 54 (10) (2007) 1740–1749.
- [19] R. Visentin, C.D. Man, Y.C. Kudva, A. Basu, C. Cobelli, Circadian variability of insulin sensitivity: physiological input for in silico artificial pancreas, *Diabetes Technol. Ther.* 17 (1) (2015) 1–7.
- [20] R. Visentin, C.D. Man, C. Cobelli, One-day Bayesian cloning of type 1 diabetes subjects: towards a single-day UVA/padova type 1 diabetes simulator, *IEEE Trans. Biomed. Eng.* 63 (2016) 2416–2424.
- [21] C. Toffanin, R. Visentin, M. Messori, F.D. Palma, L. Magni, C. Cobelli, Toward a run-to-run adaptive artificial pancreas: in silico results, *IEE Trans. Biomed. Eng.* (2017). 1–1.
- [22] A. Haidar, D. Elleri, K. Kumareswaran, L. Leelarathna, J.M. Allen, K. Caldwell, H.R. Murphy, M.R. Wilinska, C.L. Acerini, M.L. Evans, D.B. Dunger, M. Nodale, R. Hovorka, Pharmacokinetics of insulin aspart in pump-treated subjects with type 1 diabetes: reproducibility and effect of age, weight and duration of diabetes, *Diabetes Care* 36 (10) (2013) E173–e174.
- [23] F. León-Vargas, F. Garelli, H. De Battista, J. Vehí, Postprandial blood glucose control using a hybrid adaptive PD controller with insulin-on-board limitation, *Biomed. Signal Process Control* 8 (2013) 724–732.
- [24] P. Herrero, J. Bondia, C.C. Palerm, J. Vehí, P. Georgiou, N. Oliver, C. Toumazou, A simple robust method for estimating the glucose rate of appearance from mixed meals, *J. Diabetes Sci. Technol.* 6 (1) (2012) 153–162.
- [25] C. Barajas-Solano, J. Bondia, R. Calm, P. Herrero, J. Vehí, A Review of Absorption Models for Mixed Meals, in: *Proceedings of the Fifth International Conference on Advanced Technologies and Treatments for Diabetes*, 2012.
- [26] D.M. Maahs, et al., Outcome measures for artificial pancreas clinical trials: a consensus report, *Diabetes Care* 39 (7) (2016) 1175–1179.
- [27] L. Magni, et al., Evaluating the efficacy of closed-loop glucose regulation via control-variability grid analysis, *J. Diabetes Sci. Technol.* 2 (4) (2008) 630–635.
- [28] D. Boiroux, T.B. Aradóttir, K.N. rgaard, N.K. Poulsen, H. Madsen, J.B.J. rrgensen, An adaptive nonlinear basal-bolus calculator for patients with type 1 diabetes, *J. Diabetes Sci. Technol.* 11 (1) (2017) 29–36.
- [29] P. Herrero, J. Bondia, O. Adewuyi, P. Pešl, M. El-Sharkawy, M. Reddy, C. Toumazou, N. Oliver, P. Georgiou, Enhancing Automatic closed-loop glucose control in type 1 diabetes with an adaptive meal bolus calculator - in silico evaluation under intra-day variability, *Comput. Methods Progr. Biomed.* 146 (2017) 125–131.